

Weakly-Anelliptical Traveltime Analysis: Ambiguity between Subsurface and Elasticity

Björn E. Rommel

(May 2, 2023)

Running head: **Subsurface versus Elasticity**

Weakly-Anelliptical Traveltime Analysis: Ambiguity between Subsurface and Elasticity

(May 2, 2023)

Running head: **Subsurface versus Elasticity**

ABSTRACT

The building of a depth model from a single gather of seismic traveltime data is inherently ambiguous since the processing of such data can only determine a horizontal slowness component, not a vertical one. Based thereon I derive a simple algorithm that generates an infinite series of combinations of subsurface and (anisotropic) elasticity models, all of which will show nearly the same seismic response, as further demonstrated by simulating wave propagation through a model with different interface dips. This algorithm assumes, firstly, all interface dips remain constant over the distance considered and, secondly, an approximation of the elasticity model – that is, linearization of a phase velocity – valid for weak anisotropy can be used. Furthermore, when applied at the classic, and analytically solvable, case of traveltime analysis for a stack of flat layers with weak transverse isotropy, the algorithm explains theoretically the combination of anisotropy parameters that govern the non-hyperbolic term of a traveltime series: the established η and its counterpart χ for a $qPqP$ - and $qSVqSV$ -wave, respectively.

INTRODUCTION

Classical traveltime analysis – that is, analyzing traveltime over offset of seismic waves (traveltime curves) on a gather-by-gather basis – provides a horizontal slowness component, otherwise known as a ray parameter, but not a vertical one. Therefore, a classical traveltime analysis is inherently ambiguous when converting a time model – a set of traveltime curves in a gather – into a subsurface-elasticity model. Hence, the question arises as to which range of subsurface-elasticity models explains a given time model, and how best to describe that range of models.

For example, any elliptical wavefront can be morphed into other elliptical ones, even a spherical one, without changing the time model, as shown in Figure 1 (Helbig, 1983). Therefore, any nearly-elliptical wavefront can possibly be morphed into other similarly nearly-elliptical wavefronts.

To that end, I propose the mapping – a “stretch” – of a slowness (s_x, s_z) into a family of slownesses $(s_x, s_z(g))$, with g being a single arbitrary parameter. Figuratively, I stretch the slowness surface along the vertical, thus creating a family of slowness surfaces, as shown in Figure 2. From there, I can convert each slowness surface to a normal or wave surface, thus also creating a family of normal or wave surfaces, as shown in Figure 2 and 3. Admittedly, though, the elasticity, which would make a wave propagate in exactly that way, will likely not even exist physically. Hence, consider the stretch, at this point, a mathematical thought experiment.

Now, recall, anisotropic seismic processing applies mostly linearized rather than exact formulae. That is because of limited seismic bandwidth, survey geometry and noise, and the limits on accuracy imposed by those seismic and environmental conditions. Hence, I may as well linearize the above

family members of my slowness, normal and wave surfaces and, lastly, the stretch itself. As it turns out, linearizing the entire process does result in a family of physical, albeit linearized surfaces.

So, once traveltimes analysis has yielded a time model, I can map it into an infinite series of subsurface-elasticity models, all of which show (approximately) the same seismic response. Its limitations are only those of traveltimes analysis: a set of inclined weakly-anisotropic layers with possibly different, but constant interface dips, and a plane surface.

The classic traveltimes series of a wave propagating in a stack of flat layers with weak transverse isotropy can be analytically stretched. One particular anisotropy model, the “nearly-isotropic” one, equates reference and NMO velocity, and my method explains theoretically the combinations of anisotropy parameters – η (Alkhalifah and Tsvankin, 1995) and its counterpart χ for a $qPqP$ - and $qSVqSV$ -wave, respectively – governing the non-hyperbolic term.

STRETCH: DEFINITION, PROPERTIES

Slowness

Let’s do a thought experiment: maintain the horizontal slowness component, but stretch the vertical one freely. Then, a formal definition of “stretching a slowness” is

$$s_x' := s_x = \text{const} \tag{1a}$$

and

$$s_z'(s_x') := \frac{1}{\sqrt{1+g}} s_z(s_x), \tag{1b}$$

where \mathbf{s} denotes slowness and g , with $g > -1$, a “stretch parameter”. Although this definition includes an awkward denominator, it does arise naturally from another equivalent, but preferred definition, equation 3.

A positive stretch parameter decreases a vertical slowness component, a negative one increases it. Figuratively, a slowness surface is squeezed or stretched, respectively, along a vertical axis. The slowness surfaces in Figure 2 illustrate as much.

Stretching and squeezing are just opposite actions. Therefore, for the sake of simplicity, the two actions “stretch” and “squeeze” shall henceforth be subsumed into the former.

Phase Velocity and Normal Surface

Stretching a slowness, equation 1, transforms the magnitude $v(\theta)$,

$$v'(\theta') = \sqrt{\frac{1+g}{1+g\sin^2\theta}} v(\theta), \quad (2a)$$

as well as the angle θ ,

$$\tan\theta' = \sqrt{1+g} \tan\theta, \quad (2b)$$

of a phase velocity.

Note, this formula holds regardless of any symmetry. However, a symmetry angle is stretched like any phase angle, equation 2b. And since a stretch is symmetrical around the vertical – to be precise, normal to the top interface – any non-aligned symmetry will be broken.

A positive stretch parameter increases the magnitude and phase angle of a phase velocity; a negative one decreases both. The amount of stretch, however, decreases with the phase angle and vanishes for horizontal propagation. Hence, figuratively, a normal surface is stretched along the vertical axis, as shown in Figure 2.

So, Figure 2 illustrates the entire process of stretching: construct a normal surface, project this normal surface across the unit circle to construct the corresponding slowness surface, stretch this slowness surface, and project this stretched slowness surface back across the unit circle to construct the corresponding stretched normal surface.

Also, the stretched phase velocity, equation 2, opens up another, and more intuitive, definition of the stretch parameter as a normalized difference between a stretched squared phase velocity $v_z'^2$ and its original squared phase velocity v_z^2 , as observed along the vertical axis:

$$g := \frac{v_z'^2 - v_z^2}{v_z^2}. \quad (3)$$

Defining the stretch parameter based on a squared phase velocity rather than just a phase velocity will eventually lead to a version of linearized formulae that are better suited for seismic processing.

Energy Velocity and Wave Surface

If a phase velocity changes, so do the magnitude $w(\phi)$ and angle ϕ of an energy velocity: its horizontal component $w_x(\phi)$,

$$w'_x(\phi') = w_x(\phi) = \text{const}, \quad (4a)$$

remains invariant, though, and only the vertical component $w_z(\phi)$,

$$w'_z(\phi') = \sqrt{1+g} w_z(\phi), \quad (4b)$$

is multiplied by the stretch term, as proven in appendix A. Consequently, an energy angle ϕ becomes

$$\tan \phi' = \frac{1}{\sqrt{1+g}} \tan \phi. \quad (4c)$$

Figure 3 illustrates as much: invariance of a horizontal energy velocity component, and stretch of its vertical component.

SUBSURFACE MODELLING

In order to include tilted interfaces I will henceforth replace the terms vertical and horizontal with normal and parallel, respectively: all property components parallel to a top interface remain invariant, those normal to it are stretched. Effectively, I align the coordinate system with a top and top normal.

Layer Thickness

In order to compensate for an increased normal velocity component while maintaining the same traveltime I must lengthen a travelpath, but the adjustable part thereof is the layer thickness only.

That is, a layer thickness h , with

$$h' = \frac{w_z'}{w_z} h \tag{5a}$$

scales with the velocity, equation 4, (Helbig, 1983). Equivalently,

$$h' = \sqrt{1 + g} \, h. \tag{5b}$$

Figure 4 illustrates the lengthening of a layer thickness along a top normal.

Base Rotation

Consequently, a base with dip α – to be precise, opening angle between top to base – rotates, with

$$\tan \alpha' = \frac{w_z'}{w_z} \tan \alpha = \frac{h'}{h} \tan \alpha \quad (6a)$$

(Helbig, 1983) or

$$\tan \alpha' = \sqrt{1 + g} \tan \alpha, \quad (6b)$$

around the intersection point of its base and top (or surface), as also shown in Figure 4. However, parallel top and base – effectively, with zero dip angle at infinite distance – remain parallel.

So, Figure 4 illustrates the complete before- and after-stretch geometry of a layer with divergent top and base.

Base-Parallel Slowness Component

If a base rotates, so does the slowness component s_{\parallel} parallel to the base, with

$$s_{\parallel}'(\theta'; \alpha') = \frac{1}{\sqrt{1 + g \sin^2 \alpha}} s_{\parallel}(\theta; \alpha), \quad (7)$$

as proven in appendix B. The parallel slowness component remains constant for zero dip – that is, parallel top and base –, and it decreases with the “angular stretch term” $\sqrt{1 + g \sin^2 \alpha}$, that is with both the stretch parameter and the (original) reflector dip.

Figure 5 illustrate the various slowness components.

Rotating Underneath

All layers underneath a stretched layer must give space by rotating likewise, equation 6. Note, the rotation point remains the same intersection point of top and base of the stretched layer above. For an example see Figure 6.

Scaling Underneath

Since the parallel slowness component, equation 7 is fixed, and the vertical one undetermined, I suggest uniform scaling of the slowness (and subsequently velocities) with the angular stretch term. Strictly speaking, uniform scaling is but one option, but the easiest one; and applying another stretch remains possible.

Assuming uniform scaling the phase velocity,

$$v'(\theta'; \alpha') := \sqrt{1 + g \sin^2 \alpha} v(\theta; \alpha) \quad (8a)$$

or, equivalently (Helbig, 1983),

$$v'(\theta'; \alpha') = \frac{\cos \alpha}{\cos \alpha'} v(\theta; \alpha). \quad (8b)$$

Segment Length

The length d of a base segment, with

$$d' = \sqrt{1 + g \sin^2 \alpha} d, \quad (9)$$

increases in line with the geometry of top and top normal.

The lengthening can just be seen in Figures 1 and 4, but, frankly, would be more pronounced with larger dips.

Multiple Subsurface Models

Take a look at Figure 6, which illustrates the following recipe for stretching a layer as well as for rotating and scaling all layers underneath that stretched layer.

Firstly, the recipe for stretching a layer goes as follows:

- (1) If rock top and rock base are parallel, skip this step. Otherwise, calculate point O, the later rotation point, by intersecting rock top and rock base.
- (2) Select point A arbitrarily on rock top.
- (3) Define a line normal to rock top through point A (2).
- (4) Calculate a point B by intersecting that line (3) and rock base.
- (5) Define a vector \overrightarrow{AB} along that line (3) from point A (2) to point B (4) having length h_1 .
- (6) Multiply that vector \overrightarrow{AB} (5) with the stretch term $\sqrt{1+g}$, thus defining vectors \overrightarrow{AC} and \overrightarrow{BC} with lengths $h_1 + \Delta h_1$ and Δh_1 .
- (7) If rock top and rock base are parallel, the new rock base is parallel through point C (6). Otherwise, the new rock base crosses rotation point O (1) and point C (6).
- (8) Points B (4) and C (7) define equivalent (e.g., start or end) points of a segment on rock base.
- (9) If rock top and base are parallel set $\Delta\alpha := 0$. Otherwise, define opening angles $\alpha = \angle AOB$, $\alpha + \Delta\alpha = \angle AOC$ and calculate $\Delta\alpha = \arctan(\sqrt{1+g} \tan \alpha) - \alpha$.

Secondly, the recipe for rotating and scaling layers underneath continues as follows:

- (10) Define a line normal to the original rock base through point B (4).
- (11) Calculate a point D by intersecting that line (10) with target base.

- (12) Define a vector \overrightarrow{BD} from point B (4) to point D (11) having length h_2 .
- (13) Rotate that vector \overrightarrow{BD} (12) by $\Delta\alpha$ (9), thus defining a vector \overrightarrow{BE} with $\angle DBE = \Delta\alpha$.
- (14) Scale that vector \overrightarrow{BE} (13) with the angular stretch term $\sqrt{1 + g \sin^2 \alpha}$, thus defining a vector \overrightarrow{BF} with a total length of $h_2 + \Delta h_2$. That is in order to scale all dimensions uniformly.
- (15) Add to that vector \overrightarrow{BF} (14) a vector $\overrightarrow{FG} = \overrightarrow{BC}$ (6), thus defining a point G on the new target base. That is in order to make space for the stretched layer.

Alternatively, attach the foot of vector \overrightarrow{BD} at point C (7) and perform steps (13) through (14) accordingly.

Note, each layer can be stretched at will, with the layers underneath rotated and scaled accordingly. Therefore, the above process can be repeated multiple times, but the result is unfortunately neither additive nor commutative.

Wave Propagation

Wavefronts ray-traced through a stack of inclined layers are indeed invariant under stretch, as illustrated in Figure 7. In spite of extreme stretch parameters, original and stretched wavefronts, at least those of the direct and reflected waves shown, do meet at the source level (here, surface). So, the thought experiment does indeed provide a recipe for constructing a series of velocity / subsurface models each of which giving the same seismic response.

WEAKLY-ANELLIPTIC LINEARIZATION

Phase-Velocity Series

Up to this point, though, the thought experiment has disregarded physical reality: stretching an exact phase velocity, equation 2, generates another physical one only in the case of elliptical anisotropy, the case treated by Helbig (1983). However, going linearized will make all stretching physical.

So, assume a generic linearized squared phase velocity,

$$v^2(\theta) \approx v_0^2 (1 + r_2 \sin^2 \theta + r_4 \sin^4 \theta + \dots), \quad (10)$$

where $|r_2|, |r_4|, \dots \ll 1$ are a sequence of small “phase-velocity parameters.” Their particular definition does not matter: they might be numerically best-fitting or theoretical ones as, for example, Thomsen’s (1986) anisotropy parameters, as listed in Table 1. Generally, though, I prefer a generic ansatz to cover all wavetypes, to accept different kind of theoretical anisotropy parameters, and to enable accurate numerical computation.

Then, stretching, equation 2, and linearizing yields a like structured squared phase velocity. Its parameters, as derived in appendix C, are as follows:

a squared reference velocity $v_0'^2$,

$$v_0'^2 = v_0^2 (1 + g), \quad (11a)$$

a second phase-velocity parameter r_2' ,

$$r_2' = \frac{r_2 - g}{1 + g}, \quad (11b)$$

and a fourth phase-velocity parameter r_4' ,

$$r_4' = \frac{r_4}{(1 + g)^2}. \quad (11c)$$

The point being: a 3-term linearized phase velocity matches the exact one sufficiently well, stretching it is well-defined, and the resultant 3-term linearized phase velocity can be matched by other exact ones, as shown in Figure 8. Consequently, the respective traveltime curves are indistinguishable, as shown in Figure 9, provided the layer thickness is adjusted.

Note, however, the approximations: linearizing, truncating a stretch, and matching. Hence, the stretch parameter must be “small” such that a given phase-velocity series still converges and remains, in all subjectivity, sufficiently accurate for a given range of phase angles. Such a phase velocity (and the respective medium, too) shall henceforth be called “weakly anelliptical.” That is because not ellipticity, but any deviation from ellipticity, as expressed in the fourth (and higher-order) phase-velocity coefficient, equation 11c, matters as phase velocity, equation 10, and stretch, equation 11, are now approximate.

Traveltime Series

A generic traveltime series for a stack of flat layers reads (compare with Hake, Helbig and Mesdag, 1984, Tsvankin and Thomsen, 1994),

$$t^2(x) \approx c_0 + c_2x^2 + c_4x^4 + \dots, \quad (12)$$

where the “traveltime-series coefficients” c are as follows:

of 0th order or the squared two-way vertical traveltime t_0 ,

$$c_0 = \left\{ \sum_{k=1}^n t_{0k} \right\}^2 = \left\{ \sum_{k=1}^n \frac{h_k}{v_{0k}} \right\}^2 = \frac{h^2}{v_0^2} := t_0^2, \quad (13a)$$

of 2nd order or the squared inverse NMO-velocity v_{NMO} ,

$$c_2 = \frac{\sum_{k=1}^n t_{0k}}{\sum_{k=1}^n t_{0k} v_{\text{NMO}k}^2} := \frac{1}{v_{\text{NMO}}^2}, \quad (13b)$$

and of 4th order or the non-hyperbolic term,

$$c_4 = \frac{\left\{ \sum_{k=1}^n t_{0k} v_{\text{NMO}k}^2 \right\}^2 - \left\{ \sum_{k=1}^n t_{0k} \right\} \left\{ \sum_{k=1}^n t_{0k} v_{\text{NMO}k}^4 \left[1 + 4 \frac{r_{4k}}{(1 + r_{2k})^2} \right] \right\}}{4 \left\{ \sum_{k=1}^n t_{0k} v_{\text{NMO}k}^2 \right\}^4}. \quad (13c)$$

Here, t_{0k} is the one-way traveltime for the propagation of a wave along the vertical in layer k ,

$$v_{\text{NMO}k} = v_{0k} \sqrt{1 + r_{2k}} \quad (14)$$

and v_{0k} are the corresponding NMO-velocity and reference velocity, respectively, in that layer; and r_{2k} and r_{4k} are the corresponding phase-velocity parameters, as listed in Tables 1 and 2. The same properties without the layer index k refer to their respective averages over the entire stack of layers. Note, each layer k is traversed at least twice and accounted for accordingly: with the same properties for a pure-mode $\grave{q}P\acute{q}P$ - or $\grave{q}\acute{S}Vq\acute{S}V$ -wave, or with qP and qSV properties for a mode-converted $\grave{q}Pq\acute{S}V$ -wave.

Point being, the traveltime series, equation 12 through equation 13, is invariant under any stretch, equation 2. To prove invariance it is both necessary and sufficient to prove each of the

two-way vertical traveltime, the NMO-velocity and the combination $r_4/(1+r_2)^2$ of phase-velocity parameters being invariant themselves. Clearly, the vertical traveltime is indeed invariant, provided the layer thickness,

$$h_k' = h_k \sqrt{1+g}, \quad (15)$$

counters a change in the reference phase velocity. The NMO-velocity and that combination of phase-velocity parameters are also invariant, as proven in appendix E. Hence, as claimed, any one layer can be stretched, albeit within the limit of weak anellipticity, and no change in the traveltime series, equation 12, will be observed.

NEARLY-ISOTROPIC TRAVELTIME

Near-Isotropy

Classic time processing equates an NMO-velocity with a reference velocity. Effectively, it stretches a true, but non-observable reference velocity to an observable NMO-velocity, and anisotropy first appears in higher-order terms. Such a medium shall henceforth be called “nearly isotropic.”

That is, the stretch parameter, equation 3, is set to

$$g = \frac{v_{\text{NMO}}^2 - v_0^2}{v_0^2}. \quad (16)$$

For a pure-mode wave propagating in a nearly-isotropic halfspace, where the NMO-velocity, equation 14, is $v_{\text{NMO}} = v_0 \sqrt{1+r_2}$, the stretch parameter simplifies to

$$g = r_2. \quad (17)$$

Phase Velocity

Then, the linearized phase velocity, equation 10, is reduced to

$$v^{\dagger 2} \approx v_0^{\dagger 2} (1 + r_4^{\dagger} \sin^4 \theta + \dots) \quad (18)$$

with the reference velocity, equation 11a,

$$v_0^{\dagger 2} = v_0^2 (1 + r_2) = v_{\text{NMO}}^2, \quad (19a)$$

the quadratic term, equation 11b, by definition,

$$r_2^{\dagger} = 0, \quad (19b)$$

and the quartic term, equation 11c,

$$r_4^{\dagger} = \frac{r_4}{(1 + r_2)^2}, \quad (19c)$$

where a dagger “ \dagger ” shall henceforth denote near isotropy. Also, the depth,

$$h^{\dagger} = v_{\text{NMO}} t_0, \quad (19d)$$

is fixed.

Traveltime Series

Consequently, the traveltime series, equations 12 through equations 13, for a pure-mode wave in a single layer simplifies to

$$t^2 \approx t_0^2 + \frac{1}{v_{\text{NMO}}^2} x^2 - \frac{r_4^{\dagger}}{t_0^2 v_{\text{NMO}}^4} x^4 + \dots \quad (20)$$

It is characterized by only 3 independent parameters: the two-way vertical traveltime t_0 , the NMO-velocity v_{NMO} and a single phase-velocity parameter r_4^\dagger .

Up to this point the generic phase-velocity parameters hold for every wavetype. To reveal wavetype-specific features, though, those parameters shall be linked to Thomsen's (1986) anisotropy parameters; and specifically for the quartic term see Table 2.

$qPqP$ -Wave: The quartic term, equation 19c, reads

$$r_4^\dagger \approx 2 \frac{(\epsilon - \delta)}{1 + 2\delta} := 2\eta \quad (21)$$

when taking the limit for an infinitely large qP -to- qSV velocity ratio. That is, the phase-velocity parameter approaches Alkhalifah and Tsvankin's (1995) anisotropy parameter η times a factor 2, where the latter factor is simply due to the phase velocity above, equation 18, being squared. For an example see Figures 8 and 9.

$qSVqSV$ -Wave: The quartic term, equation 19c, reads

$$r_4^\dagger \approx -2 \frac{\frac{v_{P0}^2}{v_{S0}^2} (\epsilon - \delta)}{1 + 4 \frac{v_{P0}^2}{v_{S0}^2} (\epsilon - \delta)} := -2\chi, \quad (22)$$

when neglecting second-order terms in both the numerator and denominator, as listed in Table 2.

Traveltime Inversion

For sure, classical traveltime inversion of a $qPqP$ -wave does determine those three parameters and, in one of many ways published, assumes another parameter – e.g., reference velocity – to re-calculate depth and anisotropy, thus effectively stretching the medium. However, fitting a phase

velocity to a travelttime curve and performing any stretch numerically ought to be more accurate. Stretching transforms any one elasticity model – or set of phase-velocity parameters – into a range of elasticity models, as shown in Figure 10, all of which produce nearly the same travelttime curve.

CONCLUSIONS

The phase (and wave) field observed at the surface of a half-space with arbitrarily orientated plane interfaces, separating one region of space with weakly anelliptical anisotropy, is nearly invariant against transformations that result in the stretching of this region perpendicular to its top, provided the stretching is accompanied by a corresponding change in the shape of the normal (and wave) front as well as an appropriate rotating and scaling of dimensions (thicknesses) and a uniform scaling of velocities below that transformed region in case of divergent top and base (modifying Helbig’s (1983) lemma).

To realize such a transformation of subsurface and phase- / wavefront geometries I propose a “stretch” process: it, firstly, provides a recipe for constructing a transformed subsurface and, secondly, provides the formula for calculating a transformed phase velocity. Strictly speaking, the exact version of that formula creates a physically impossible phase velocity (unless the anisotropy is elliptical), but after linearizing the entire stretch process an approximate version does create a physically possible linearized phase velocity. That is provided the anisotropy is weakly anelliptical, the range of incidence angles is small, and the stretch parameter is small. In this way, the stretch process creates a range of subsurface-elasticity models, all of which show nearly the same travelttime curve. The invariance is demonstrated numerically and also proven analytically for a stack of flat layers with VTI.

APPENDIX A

ENERGY VELOCITY

Definition: The horizontal and vertical energy velocity components are (Berryman, 1979)

$$w_x = v \sin \theta + \frac{\partial v}{\partial \theta} \cos \theta \quad (\text{A-1a})$$

and

$$w_z = v \cos \theta - \frac{\partial v}{\partial \theta} \sin \theta, \quad (\text{A-1b})$$

respectively.

Horizontal Component: Starting with a stretched horizontal energy velocity component,

$$w'_x(\theta') = v'(\theta') \sin \theta' + \frac{\partial v'(\theta')}{\partial \theta'} \cos \theta', \quad (\text{A-2a})$$

replacing the stretched phase velocity, equation 2a, executing the differentiation, equation F-1, and replacing the trigonometric functions, equations G-1 and G-2, I obtain

$$w'_x(\theta') = v(\theta) \sin \theta + \frac{\partial v(\theta)}{\partial \theta} \cos \theta, \quad (\text{A-2b})$$

which, in turn, matches the very definition, equation A-1a:

$$w'_x(\theta') = w_x(\theta). \quad (\text{A-2c})$$

That is, the horizontal component is invariant under stretch.

Vertical Component: In a similar way, the stretched vertical energy velocity component turns into

$$w'_z(\theta') = \sqrt{1+g} \left(v(\theta) \cos \theta - \frac{\partial v(\theta)}{\partial \theta} \sin \theta \right), \quad (\text{A-3a})$$

which matches the very definition, equation A-1b, times the stretch term:

$$w'_z(\theta') = \sqrt{1+g} w_z(\theta). \quad (\text{A-3b})$$

That is, the stretched vertical component of a energy velocity simply equals the original one times the stretch term.

APPENDIX B

PARALLEL SLOWNESS COMPONENT

Start with the parallel slowness component in a rotated coordinate system,

$$s'_{\parallel}(\alpha') = s'_x \cos \alpha' - s'_z \sin \alpha', \quad (\text{B-1a})$$

replace the stretched slowness and trigonometric functions, equations 1 and equations G-1 through G-2, respectively,

$$s'_{\parallel}(\alpha') = \frac{1}{\sqrt{1+g \sin^2 \alpha}} (s_x \cos \alpha - s_z \sin \alpha), \quad (\text{B-1b})$$

to obtain

$$s'_{\parallel}(\alpha') = \frac{1}{\sqrt{1+g \sin^2 \alpha}} s_{\parallel}(\alpha). \quad (\text{B-1c})$$

APPENDIX C

PHASE-VELOCITY PARAMETERS

Definition: Assume a generic linearized squared phase velocity series:

$$v^2(\theta) \approx v_0^2 (1 + r_1 \sin \theta + r_2 \sin^2 \theta + \dots) \quad (\text{C-1})$$

with $|r_i| \ll 1$ for $i = 1, 2, \dots$

The stretch, equation 2a itself does not transform the original phase angle to the stretched one; instead, I first invert the stretched phase angle, equation 2b, and express

$$\sin \theta = \sin \left[\arctan \left[\frac{1}{\sqrt{1+g}} \tan \theta' \right] \right] \quad (\text{C-2a})$$

$$= \sqrt{\frac{1}{1+g - g \sin^2 \theta'}} \sin \theta'. \quad (\text{C-2b})$$

Then, starting with the definition of the stretched phase velocity, equation 2a, inserting the linearized phase velocity, equation C-1, replacing all sines, equation C-2b, and expanding I obtain a like-structured equation with the reference velocity,

$$v_0'^2 = v_0^2 (1 + g), \quad (\text{C-3a})$$

and the first four stretched phase-velocity parameters,

$$r_1' = \frac{r_1}{(1+g)^{1/2}}, \quad (\text{C-3b})$$

$$r_2' = \frac{r_2 - g}{1+g}, \quad (\text{C-3c})$$

$$r_3' = \frac{2r_3 - r_1 g}{2(1+g)^{3/2}} \quad (\text{C-3d})$$

and

$$r_4' = \frac{r_4}{(1+g)^2}, \quad (\text{C-3e})$$

respectively.

Note, the medium might show a symmetry axis that is not aligned with the stretch axis. The corresponding symmetry angle is transformed like any phase angle, equation 2b. However, such a tilted squared phase velocity series

$$v^2(\theta; \theta_0) \approx v_0^2. \quad (C-4)$$

$$\left[1 + \sum_{i=1}^{\infty} r_i \sin^i(\theta - \theta_0) + \dots \right]$$

with $|r_i| \ll 1$ for $i = 1, 2, \dots$

with a symmetry angle θ_0 turns at best into

$$v'^2(\theta'; \theta_0') \approx (1 + g \cos^2 \theta'). \quad (\text{C-5a})$$

$$\left\{ 1 + \sum_{n=1} f^n r_n \sin^n(\theta' - \theta_0') \right\}$$

with

$$f = \frac{\sqrt{1+g}}{\sqrt{1+g \cos^2 \theta'} \sqrt{1+g \cos^2 \theta_0'}} \quad (\text{C-5b})$$

with mixed sines in terms of the phase and symmetry angles.

APPENDIX D

TRAVELTIME-SERIES COEFFICIENTS

Generic Traveltime Series: The quadratic and quartic coefficients of a generic traveltime series, equation 13, are

$$c_2 = \lim_{x \rightarrow 0} \frac{\sum_{k=1}^n \Delta t_k}{\sum_{k=1}^n \Delta t_k V_k^2} \quad (\text{D-1a})$$

and

$$c_4 = \lim_{x \rightarrow 0} \frac{\left\{ \sum_{k=1}^n \Delta t_k V_k^2 \right\}^2 - \left\{ \sum_{k=1}^n \Delta t_k \right\} \left\{ \sum_{k=1}^n \Delta t_k (V_k^4 + H_k) \right\}}{4 \left\{ \sum_{k=1}^n \Delta t_k V_k^2 \right\}^4} \quad (\text{D-1b})$$

with the V-term

$$V_k^2 = \frac{w_{kx}}{s_{kx}} = \frac{w_k \sin \phi_k}{\frac{\sin \theta_k}{v_k}} \quad (\text{D-2a})$$

and the H-term

$$H_k = \frac{1}{s_x} \frac{\partial V_k^2}{\partial s_x}, \quad (\text{D-2b})$$

where Δt_k denotes the interval traveltime, ϕ_k the energy angle and w_k the magnitude of the energy velocity of a wave propagating one-way in layer k (Hake, Helbig and Mesdag, 1984).

Inserting the energy velocity,

$$w = \sqrt{v^2 + \left(\frac{\partial v}{\partial \theta} \right)^2}, \quad (\text{D-3a})$$

and angle,

$$\tan \phi = \frac{\tan \theta + \frac{1}{v} \frac{\partial v}{\partial \theta}}{1 - \tan \theta \frac{1}{v} \frac{\partial v}{\partial \theta}}, \quad (\text{D-3b})$$

(Berryman, 1979) into the V-term above, equation D-2a, yields eventually the following still generic,

but short expression:

$$V_k^2 = v_k^2 \left(1 + \frac{1}{\tan \theta_k} \frac{1}{v_k} \frac{\partial v_k}{\partial \theta_k} \right). \quad (\text{D-4})$$

VTI: Inserting a linearized phase velocity, equation 10, which holds specifically for a VTI medium, yields

$$V_k^2 \approx v_{0k}^2 (1 + r_{2k} + 2r_{4k} \sin^2 \theta_k - r_{4k} \sin^4 \theta_k + \dots) \quad (\text{D-5a})$$

in terms of the phase angle or

$$\approx v_{0k}^2 (1 + r_{2k} + 2r_{4k} s_x^2 v_{0k}^2 - (1 - 2r_{2k}) r_{4k} s_x^4 v_{0k}^4 + \dots) \quad (\text{D-5b})$$

in terms of the horizontal slowness component.

Inserting the latter V-term, equation D-5b, into the H-term, equation D-2b, yields

$$H_k \approx v_{0k}^4 (4r_{4k} - 4(1 - 2r_{2k}) r_{4k} s_x^2 v_{0k}^2 + \dots) \quad (\text{D-6a})$$

in terms of the horizontal slowness component or

$$\approx v_{0k}^4 (4r_{4k} - 4(1 - 2r_{2k}) r_{4k} \sin^2 \theta + 4r_{2k} (1 - 2r_{2k}) r_{4k} \sin^4 \theta + \dots) \quad (\text{D-6b})$$

in terms of the phase angle.

Vertical Incidence: Calculating both terms, equations D-5a and D-6b, respectively, for zero incidence angle yields

$$V_k^2(0^\circ) = v_{0k}^2 (1 + r_{2k}) = v_{\text{NMO}k}^2 \quad (\text{D-7a})$$

and

$$H_k(0^\circ) = 4r_{4k} v_{0k}^4 = 4 \frac{r_{4k}}{(1 + r_{2k})^2} v_{\text{NMO}k}^4. \quad (\text{D-7b})$$

The V-term turns out to be the squared NMO-velocity, and the H-term includes the frequently occurring combination of phase-velocity parameters $r_4/(1 + r_2)^2$.

Lastly, inserting those two terms, equations D-7a and D-7b, into the generic traveltime series, equation D-1, gives the second and fourth-order coefficients c_2 and c_4 , equations 13b and 13c, shown above. Therein, the limit of the interval traveltime for zero offset, $\lim_{x \rightarrow 0} \Delta t$, is, of course, simply the one-way vertical traveltime t_0 .

APPENDIX E

TRAVELTIME-SERIES INVARIANCE

As said above, any kinematic property is assumed to be invariant under stretching. Inspecting the coefficients, equations 13a through 13c, of the traveltime series closely, it is sufficient to prove the following three properties to be invariant: the vertical traveltime t_0 , the NMO-velocity v_{NMO} and the combination $r_4/(1+r_2)^2$ of phase-velocity parameters.

Vertical Traveltime: The vertical traveltime itself,

$$t_0' = \frac{h'}{v_0'} \tag{E-1a}$$

$$= \frac{h\sqrt{1+g}}{v_0\sqrt{1+g}} \tag{E-1b}$$

$$= t_0, \tag{E-1c}$$

is constant, provided the layer thickness,

$$h' = h\sqrt{1+g}, \tag{E-2}$$

is adjusted to counter the change in the reference phase velocity.

NMO-Velcoity: The NMO-velocity

$$v_{\text{NMO}}'^2 = v_0'^2 (1 + r_2') \quad (\text{E-3a})$$

$$= v_0'^2 (1 + g) \left(1 + \frac{r_2 - g}{1 + g} \right) \quad (\text{E-3b})$$

$$= v_0'^2 (1 + r_2) = v_{\text{NMO}}'^2, \quad (\text{E-3c})$$

is also invariant.

$\mathbf{r}_4/(\mathbf{1} + \mathbf{r}_2)^2$: In the same way, this combination of phase-velocity parameters is proven to be invariant.

APPENDIX F

DERIVATIVES OF THE PHASE VELOCITY

First Derivative: Hence, substituting a stretched phase angle with the original one and applying the chain rule yields

$$\frac{\partial v'(\theta')}{\partial \theta'} = \frac{\frac{\partial v'(\theta)}{\partial \theta}}{1} \frac{1}{\frac{\partial \theta'}{\partial \theta}}. \quad (\text{F-1a})$$

Replacing the stretched phase velocity, equation 2a, and angle, equation 2b,

$$= \frac{\partial \sqrt{\frac{1+g}{1+g \sin^2 \theta}} v(\theta)}{\partial \theta} \frac{1}{\frac{\partial \arctan [\sqrt{1+g} \tan \theta]}{\partial \theta}}, \quad (\text{F-1b})$$

and executing the differentiations gives

$$= \frac{-g \sin \theta \cos \theta}{\sqrt{1+g \sin^2 \theta}} v(\theta) + \sqrt{1+g \sin^2 \theta} \frac{\partial v(\theta)}{\partial \theta}. \quad (\text{F-1c})$$

Second Derivative: Similarly,

$$\begin{aligned} \frac{\partial^2 v'(\theta')}{\partial \theta'^2} &= \frac{g(\sin^2 \theta - \cos^2 \theta + g \sin^4 \theta)}{\sqrt{1+g}\sqrt{1+g \sin^2 \theta}} v(\theta) + \\ &\quad \frac{\sqrt{1+g \sin^2 \theta}}{\sqrt{1+g}} \frac{\partial^2 v(\theta)}{\partial \theta^2}. \end{aligned} \quad (\text{F-2})$$

APPENDIX G

TRIGONOMETRIC FUNCTIONS

Sine: The sine of any angle transforms as follows:

$$\sin \theta' = \sin \left[\arctan \left[\sqrt{1+g} \tan \theta \right] \right] \quad (\text{G-1a})$$

$$= \sqrt{\frac{1+g}{1+g \sin^2 \theta}} \sin \theta. \quad (\text{G-1b})$$

Cosine: Similarly, the cosine transforms as follows:

$$\cos \theta' = \sqrt{\frac{1}{1+g \sin^2 \theta}} \cos \theta. \quad (\text{G-2})$$

REFERENCES

- Alkhalifah, T., and I. Tsvankin, 1995, Velocity analysis for transversely isotropic media: *GEOPHYSICS*, **60**, 1550–1566.
- Berryman, J. G., 1979, Long-wave elastic anisotropy in transversely isotropic media: *GEOPHYSICS*, **44**, 896-917.
- Hake, H., K. Helbig, and C. S. Mesdag, 1984, Three-term Taylor series for $t^2 - x^2$ curves over layered transversely isotropic ground: *GEOPHYSICAL PROSPECTING*, **32**, 828-850.

Helbig, K., 1983, Elliptical anisotropy - its significance and meaning: *GEOPHYSICS*, **48**, 825-832.

Thomsen, L., 1986, Weak elastic anisotropy: *GEOPHYSICS*, **51**, 1954-1966.

Tsvankin, I., and L. Thomsen, 1992, Nonhyperbolic reflection moveout in anisotropic media: *GEOPHYSICS*, **59**, 1290-1304.

Tsvankin, I., 1995, Normal moveout from dipping reflectors in anisotropic media: *GEOPHYSICS*, **60**, 268-284.

LIST OF FIGURES

- 1 Stretching an elliptical wavefront (original Helbig, 1983): Any elliptical wavefront can be arbitrarily stretched along its vertical axis; then, a wavefront in a layer underneath is scaled, and the layer itself is rotated. A prime shall henceforth denote a stretched property, λ a vertical-to-horizontal velocity ratio, α a dip angle, and d a segment length along the base. 31

- 2 Stretching a slowness and normal surface: A black curve depicts a unit circle. Outside the unit circle green and blue curves depict an original and stretched normal surface, respectively; inside the unit circle like-colored curves depict the respective slowness surfaces. Stretching works as follows: (1) select an arbitrary point A on the original normal surface; (2) project point A across the unit circle thus creating a point B on the corresponding slowness surface; (3) squeeze the vertical slowness component thus creating a point C on the stretched slowness surface; and (4) project point C across the unit circle thus creating a point D on the corresponding stretched normal surface. 32

- 3 Stretching a wave surface: The green and blue curves depict the original and stretched wave surfaces corresponding to the respective normal and slowness surfaces of Figure 2. Indeed, a wave surface can be geometrically constructed from a normal surface (not shown; see Berryman (1979)). Points A and D on the original and stretched normal surfaces, as depicted in Figure 2, are mapped onto points E and F, respectively, on the wave surfaces. Note, their horizontal coordinates remain invariant under stretch. 33

- 4 Thickness of a layer: The before- and after-stretch top, bases and top normals are depicted in green and blue, respectively. Note, stretching does not affect a top, but lengthens a top normal downwards. Hence, a layer thickness h , as measured along the top normal, is increased by Δh . Subsequently, a base rotates from a dip angle α to α' around the intersection point of top and bases. Note, this intersection point can be an imaginary one if top and base do not intersect within the offset considered, and it becomes nonsensical beyond. 34

- 5 Slowness at an interface: Assume an interface with before- and after-stretch dip angles α and α' and a wave being reflected with phase angle θ and θ' , respectively. Its parallel slowness component s_{\parallel} decreases upon stretch-induced rotation such that, firstly, the horizontal slowness component s_x remains invariant and, secondly, the vertical one s_z is reduced by the stretch term. 35

- 6 Constructing stretched and rotated / scaled layers: For the sake of simplicity the layers are, here, named overburden, rock and target. Also, the rock shall be stretched, and the target shall be rotated and scaled accordingly. The recipes are outlined in the section of multiple subsurface models; and all symbols are detailed there. 36

- 7 Wavefronts propagating in equivalent subsurface models: The subsurface model consists, here, of a surface and three layers, where the first and second layers are stretched by 0.3 and 0.1, respectively. The original and transformed interfaces are depicted with black solid and dashed lines, respectively. The source at the surface is depicted as a red star. The wavefronts shown propagate downwards to the lowermost base or upwards therefrom to the surface; only direct and pure-mode reflected waves are shown. Original and stretched wavefronts are depicted with solid and dashed lines, respectively, with colors encoding different traveltimes. Note, the surface locations of each set of original and stretched wavefronts are on top of each other for each travelttime. The insert enlarges the latest wavefront shown in green in the top right corner. 37

- 8 Stretching a phase velocity: The blue-, green-, red- and violet-colored curves depict (a) the exact phase velocity of a qP -wave, (b) its 3-term linearized phase velocity corresponding to curve (a) for incidence angles up to 40° , (c) its approximately stretched and now nearly isotropic 3-term linearized phase velocity corresponding to curve (b), and (d) its exact phase velocity reconstructed from curve (c) with the same qP -to- qSV velocity ratio. The original parameters are for Dog Creek Shale (Thomsen, 1986). Note, the exact before- and after-stretch phase velocities do not necessarily coincide in the horizontal direction, but, in practice, only a limited range of phase angles is used anyway. 38
- 9 Traveltime curves: Assume a $qPqP$ -wave propagating in a flat layer with stretch-adapted thickness. The green- and red-colored curves depict approximate traveltime curves for the respective phase velocities shown in Figure 8, whereas the exact traveltime curves are hidden underneath. Note, the approximate traveltime curves do deviate slightly the larger the incidence angle. Whether that deviation – here, maximal 0.8% – is sufficiently small depends on layer thickness and seismic bandwidth. 39
- 10 Range of seismically equivalent media: An exemplary combinations of reference velocity, second and fourth anisotropy parameters that are seismically equivalent to Dog Creek Shale (Thomsen, 1986) are depicted with a blue line. Here, the stretch parameters ranges from -0.1 to $+0.3$; combinations, which are generated by stretching in increments of 0.05 , are marked as blue points. The orange, green, and red points are projections of those points onto the (r_2, r_4) , (r_4, v) and (r_2, v) sidewalls, respectively, of the cube. A stretch of 0.2 makes the medium nearly-isotropic. 40

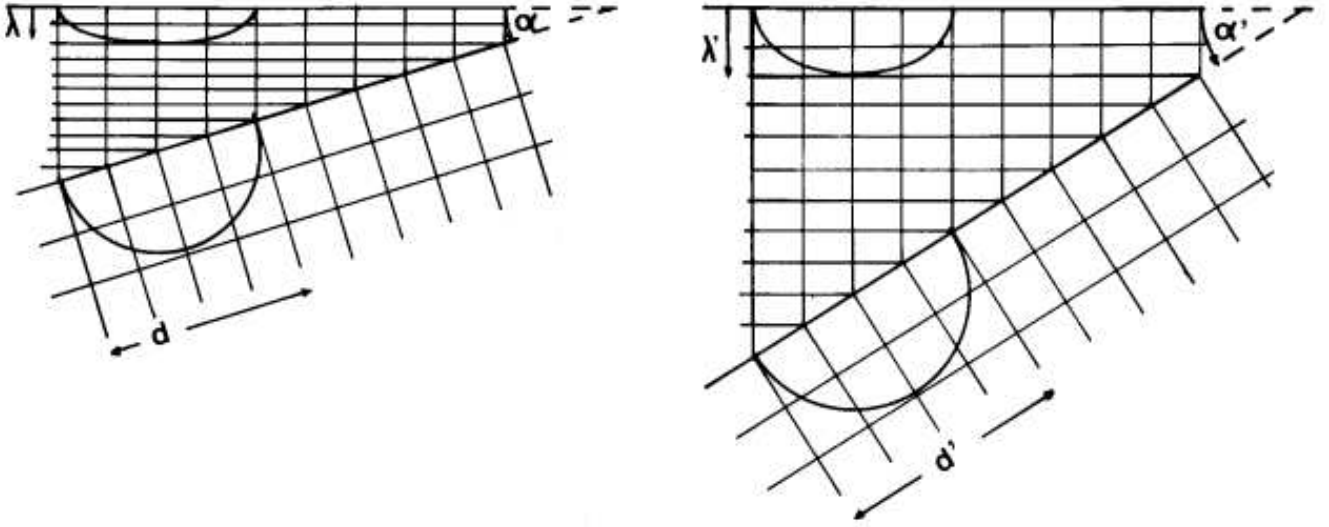


Figure 1: Stretching an elliptical wavefront (original Helbig, 1983): Any elliptical wavefront can be arbitrarily stretched along its vertical axis; then, a wavefront in a layer underneath is scaled, and the layer itself is rotated. A prime shall henceforth denote a stretched property, λ a vertical-to-horizontal velocity ratio, α a dip angle, and d a segment length along the base.

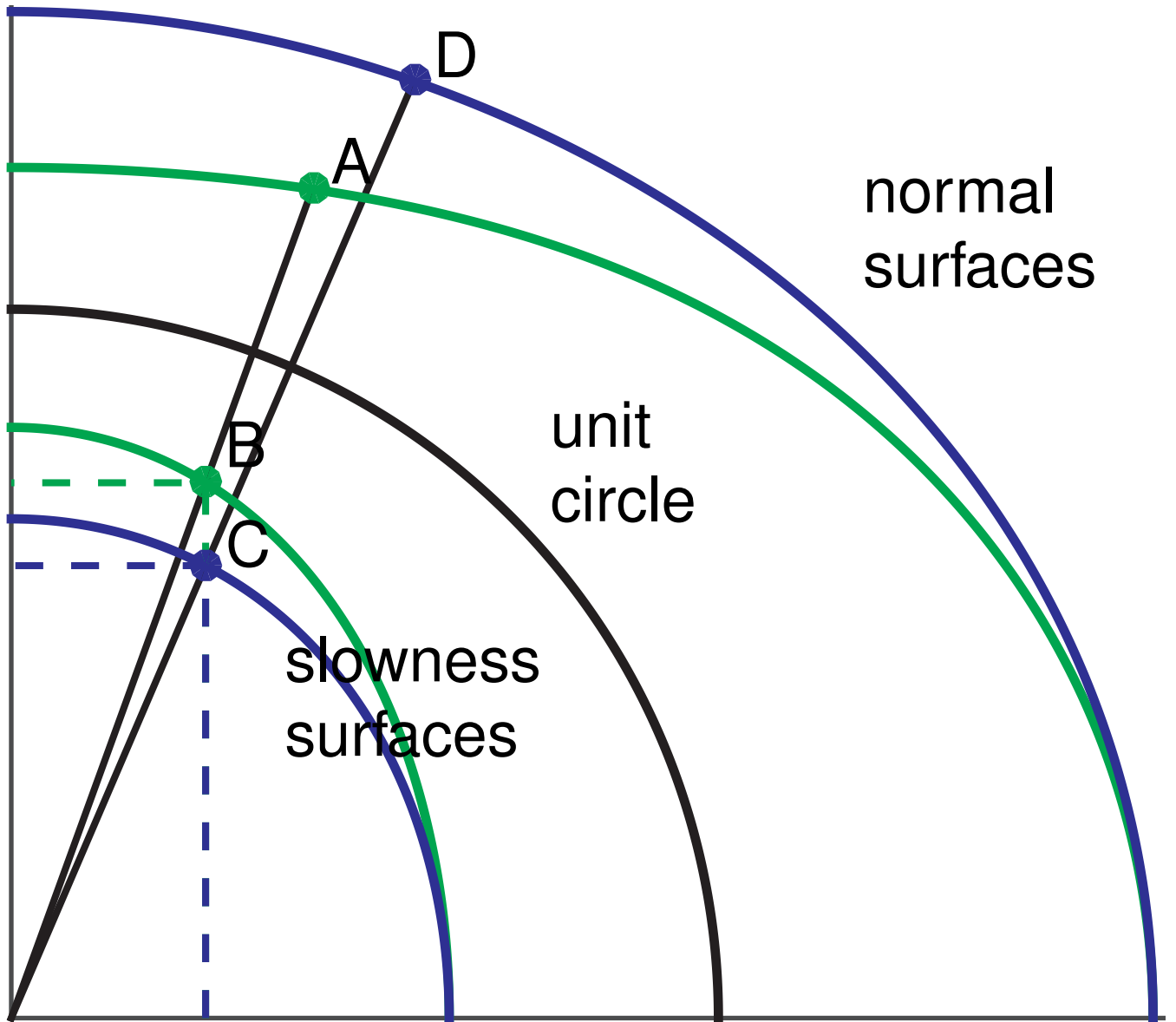


Figure 2: Stretching a slowness and normal surface: A black curve depicts a unit circle. Outside the unit circle green and blue curves depict an original and stretched normal surface, respectively; inside the unit circle like-colored curves depict the respective slowness surfaces. Stretching works as follows: (1) select an arbitrary point A on the original normal surface; (2) project point A across the unit circle thus creating a point B on the corresponding slowness surface; (3) squeeze the vertical slowness component thus creating a point C on the stretched slowness surface; and (4) project point C across the unit circle thus creating a point D on the corresponding stretched normal surface.

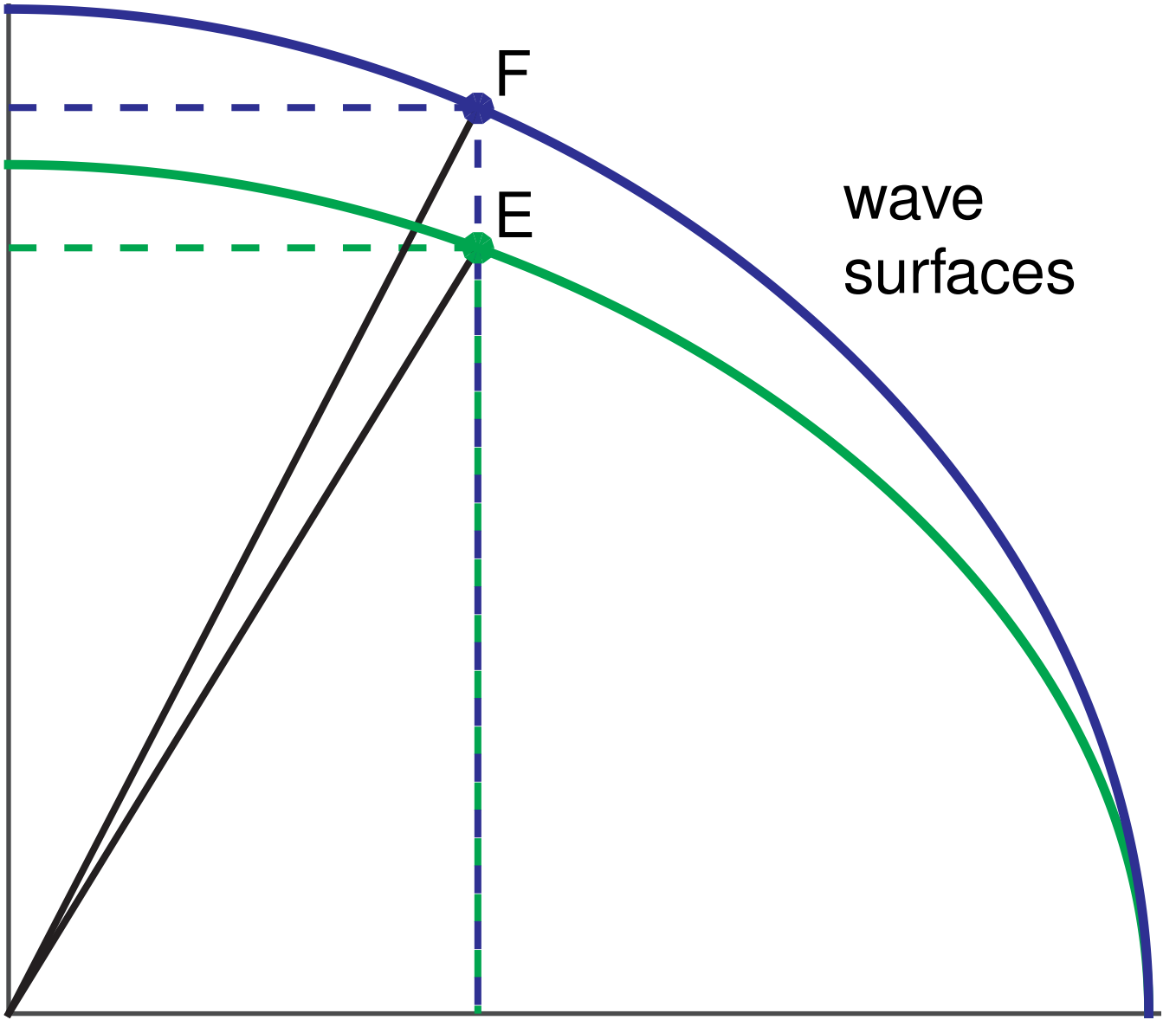


Figure 3: Stretching a wave surface: The green and blue curves depict the original and stretched wave surfaces corresponding to the respective normal and slowness surfaces of Figure 2. Indeed, a wave surface can be geometrically constructed from a normal surface (not shown; see Berryman (1979)). Points A and D on the original and stretched normal surfaces, as depicted in Figure 2, are mapped onto points E and F, respectively, on the wave surfaces. Note, their horizontal coordinates remain invariant under stretch.

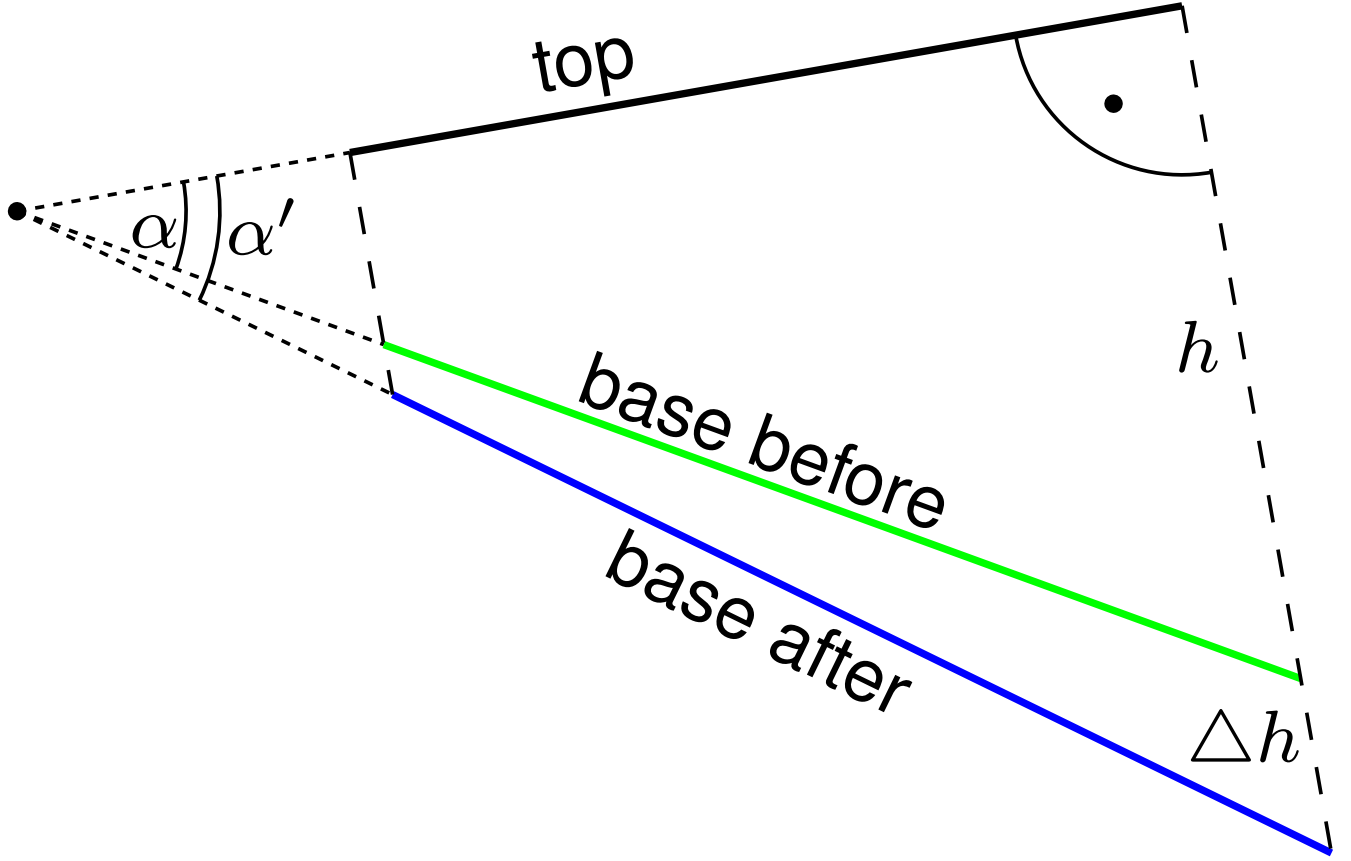


Figure 4: Thickness of a layer: The before- and after-stretch top, bases and top normals are depicted in green and blue, respectively. Note, stretching does not affect a top, but lengthens a top normal downwards. Hence, a layer thickness h , as measured along the top normal, is increased by Δh . Subsequently, a base rotates from a dip angle α to α' around the intersection point of top and bases. Note, this intersection point can be an imaginary one if top and base do not intersect within the offset considered, and it becomes nonsensical beyond.

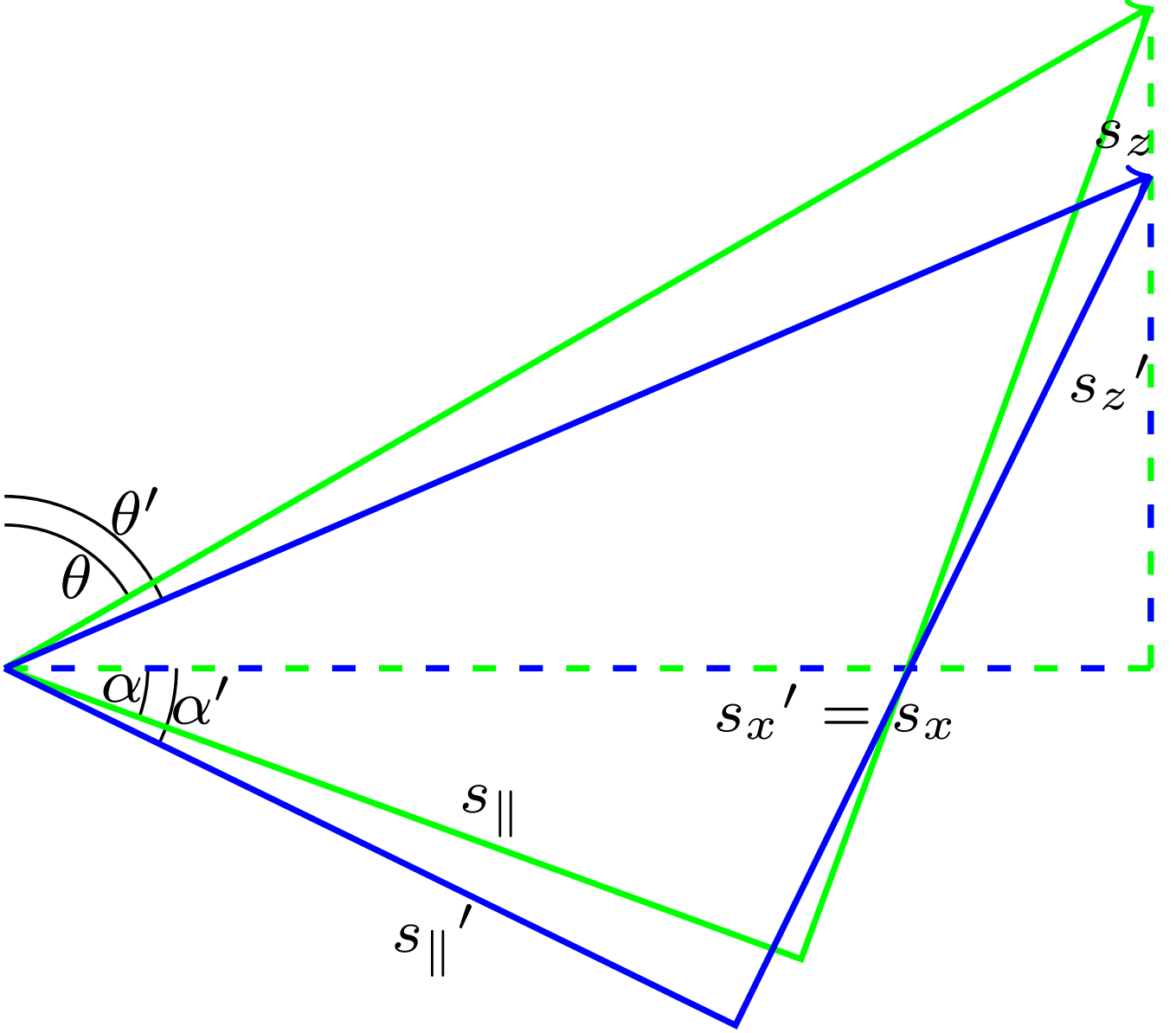


Figure 5: Slowness at an interface: Assume an interface with before- and after-stretch dip angles α and α' and a wave being reflected with phase angle θ and θ' , respectively. Its parallel slowness component $s_{||}$ decreases upon stretch-induced rotation such that, firstly, the horizontal slowness component s_x remains invariant and, secondly, the vertical one s_z is reduced by the stretch term.

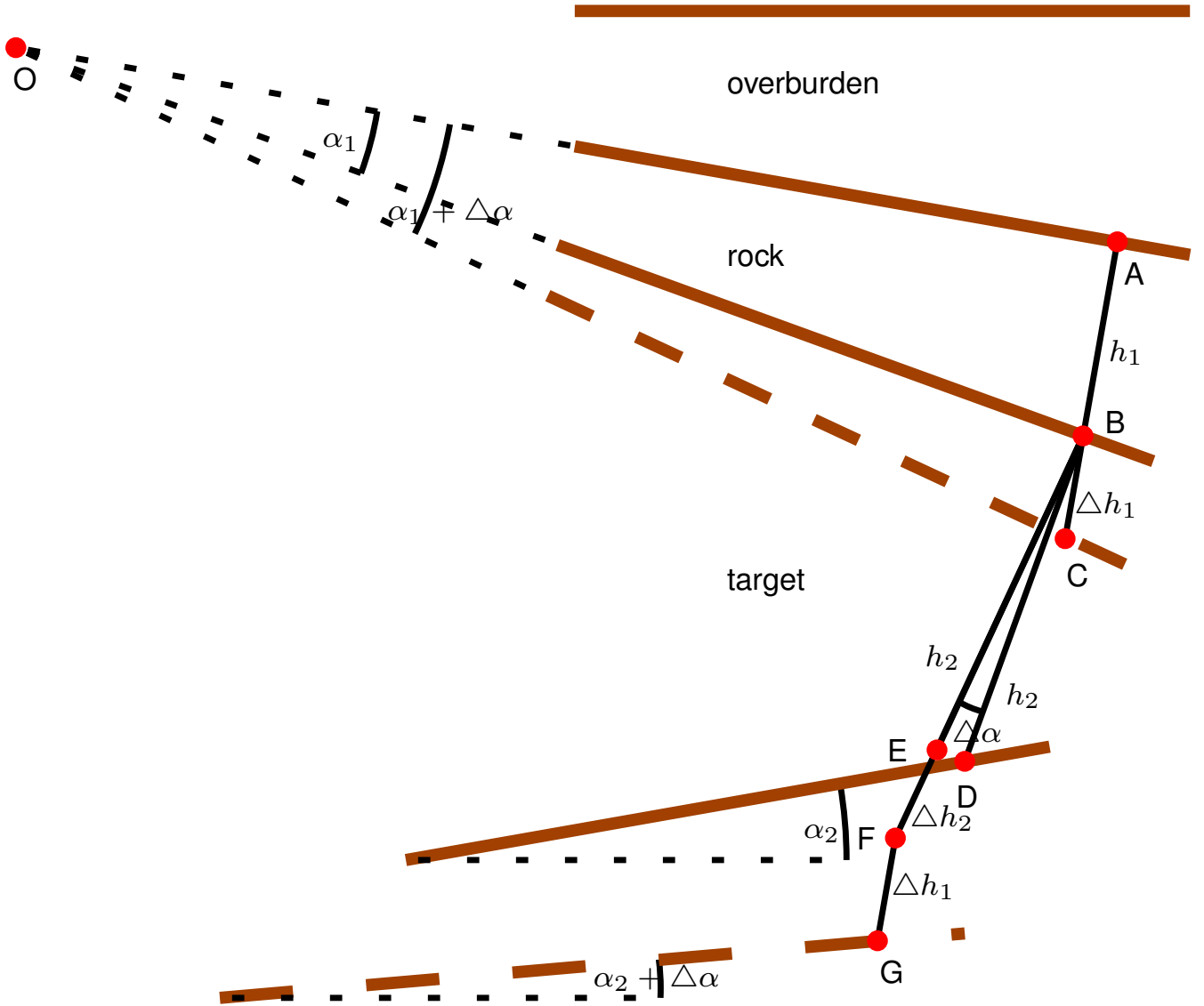


Figure 6: Constructing stretched and rotated / scaled layers: For the sake of simplicity the layers are, here, named overburden, rock and target. Also, the rock shall be stretched, and the target shall be rotated and scaled accordingly. The recipes are outlined in the section of multiple subsurface models; and all symbols are detailed there.

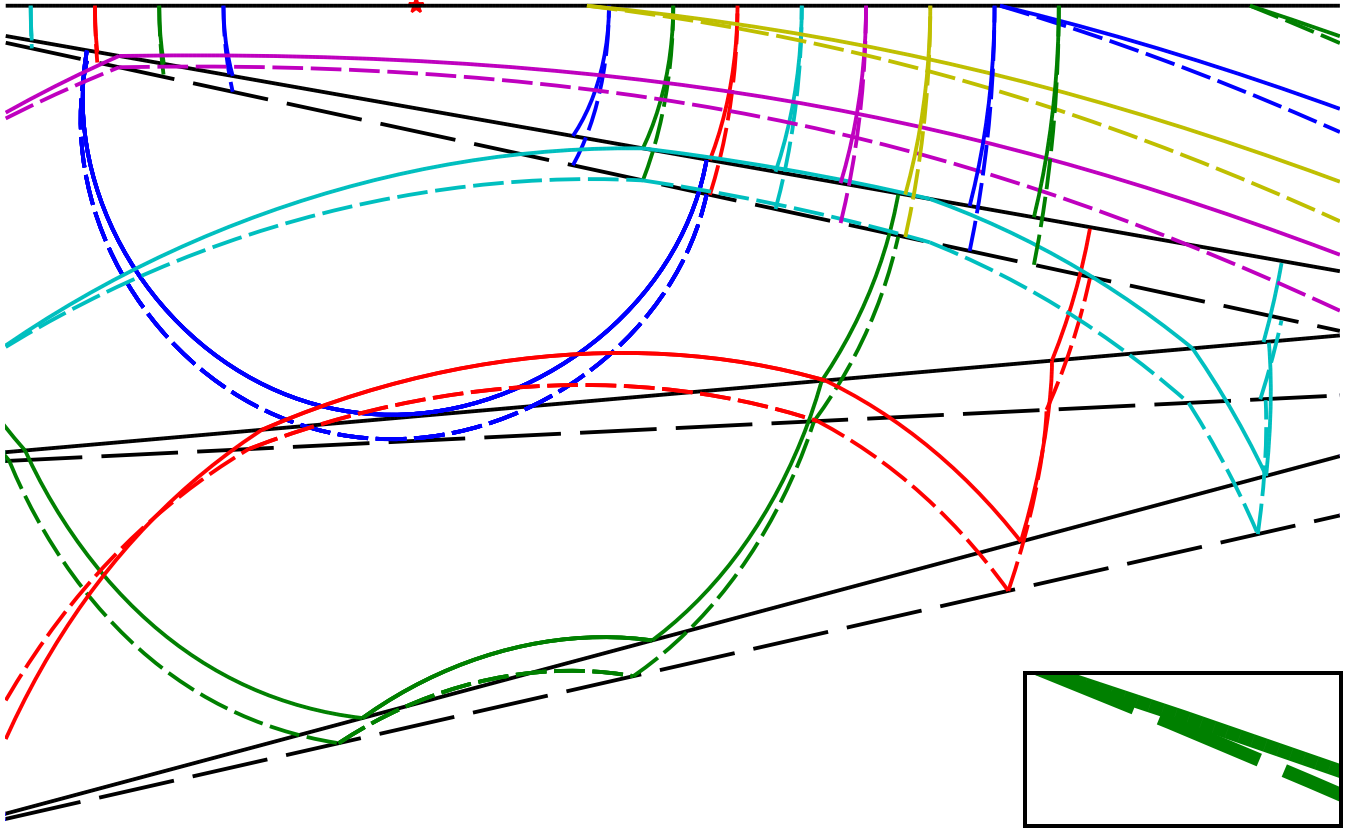


Figure 7: Wavefronts propagating in equivalent subsurface models: The subsurface model consists, here, of a surface and three layers, where the first and second layers are stretched by 0.3 and 0.1, respectively. The original and transformed interfaces are depicted with black solid and dashed lines, respectively. The source at the surface is depicted as a red star. The wavefronts shown propagate downwards to the lowermost base or upwards therefrom to the surface; only direct and pure-mode reflected waves are shown. Original and stretched wavefronts are depicted with solid and dashed lines, respectively, with colors encoding different traveltimes. Note, the surface locations of each set of original and stretched wavefronts are on top of each other for each traveltime. The insert enlarges the latest wavefront shown in green in the top right corner.

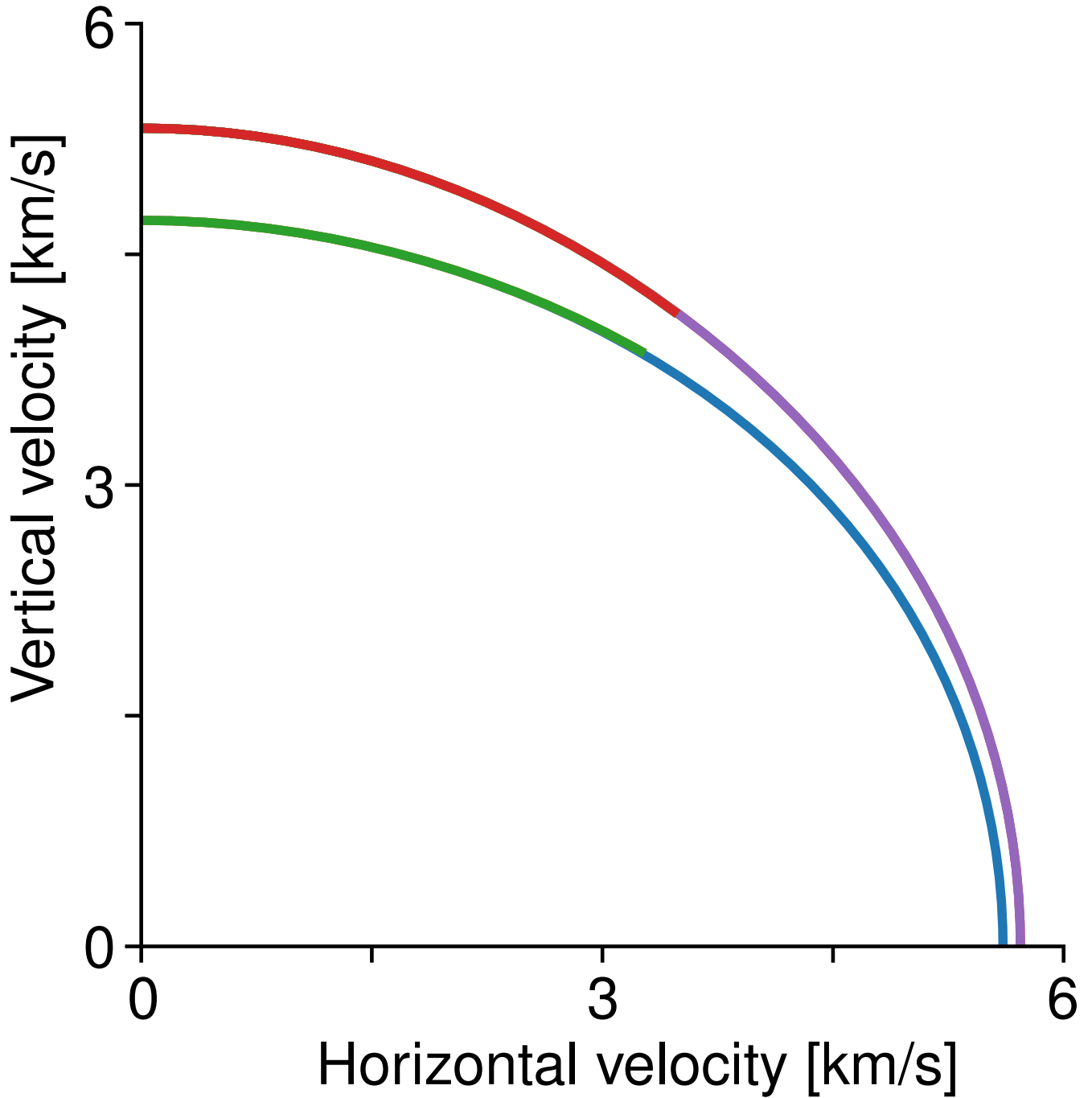


Figure 8: Stretching a phase velocity: The blue-, green-, red- and violet-colored curves depict (a) the exact phase velocity of a qP -wave, (b) its 3-term linearized phase velocity corresponding to curve (a) for incidence angles up to 40° , (c) its approximately stretched and now nearly isotropic 3-term linearized phase velocity corresponding to curve (b), and (d) its exact phase velocity reconstructed from curve (c) with the same qP -to- qSV velocity ratio. The original parameters are for Dog Creek Shale (Thomsen, 1986). Note, the exact before- and after-stretch phase velocities do not necessarily coincide in the horizontal direction, but, in practice, only a limited range of phase angles is used anyway.

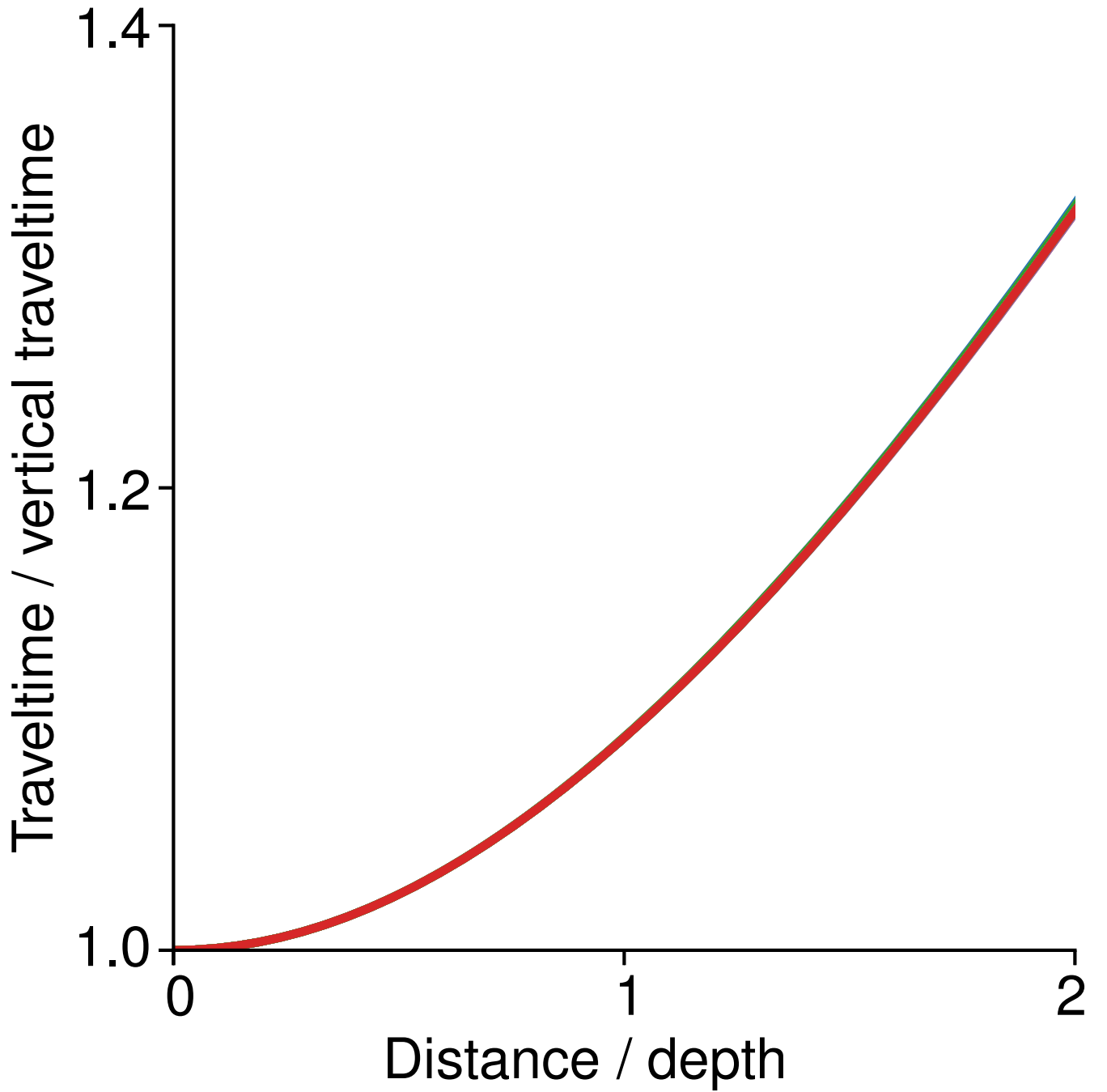


Figure 9: Traveltime curves: Assume a $qPqP$ -wave propagating in a flat layer with stretch-adapted thickness. The green- and red-colored curves depict approximate traveltime curves for the respective phase velocities shown in Figure 8, whereas the exact traveltime curves are hidden underneath. Note, the approximate traveltime curves do deviate slightly the larger the incidence angle. Whether that deviation – here, maximal 0.8% – is sufficiently small depends on layer thickness and seismic bandwidth.

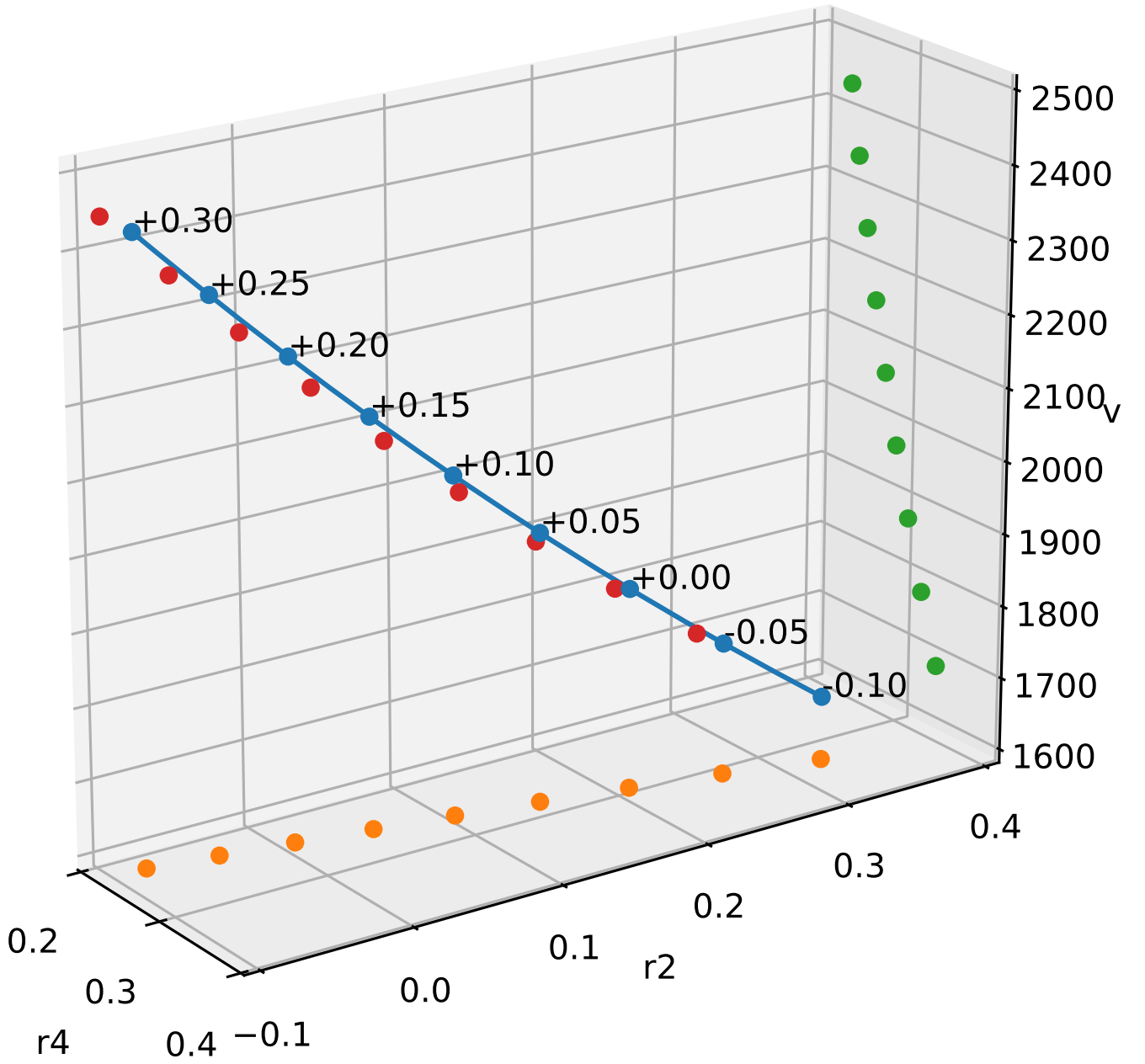


Figure 10: Range of seismically equivalent media: An exemplary combinations of reference velocity, second and fourth anisotropy parameters that are seismically equivalent to Dog Creek Shale (Thomsen, 1986) are depicted with a blue line. Here, the stretch parameters ranges from -0.1 to $+0.3$; combinations, which are generated by stretching in increments of 0.05 , are marked as blue points. The orange, green, and red points are projections of those points onto the (r_2, r_4) , (r_4, v) and (r_2, v) sidewalls, respectively, of the cube. A stretch of 0.2 makes the medium nearly-isotropic.

LIST OF TABLES

1	Phase-velocity parameters in Thomsen's notation. The parameters r_2 and r_4 of the phase-velocity series can be replaced wavetype-specifically by Thomsen's (1986) anisotropy parameters ϵ and δ and the ratio of the qP -to- qSV reference phase velocities (Thomsen, 1986; Tsvankin and Thomsen, 1994).	42
2	Phase-velocity parameters of a nearly-isotropic medium in Thomsen's notation: The quadratic term r_2^\dagger vanishes by definition, and the quartic term r_4^\dagger is governed by Thomsen's (1986) anisotropy parameters and the qP -to- qSV ratio of the reference phase velocities. Note Tsvankin and Alkhalifah's (1995) anisotropy parameter η and its newly defined counterpart χ for the $q\acute{S}Vq\acute{S}V$ -wave. Alternatively, select specific ratios of the qP -to- qSV phase velocities or apply Taylor-expansions differently. . . .	43

parameter	wavetype	
	qP	qSV
r_2	2δ	$2\frac{v_{P0}^2}{v_{S0}^2}(\epsilon - \delta)$
r_4	$2(\epsilon - \delta)\left(1 + 2\frac{v_{P0}^2}{v_{P0}^2 - v_{S0}^2}\delta\right)$	$-2\frac{v_{P0}^2}{v_{S0}^2}(\epsilon - \delta)\left(1 + 2\frac{v_{P0}^2}{v_{P0}^2 - v_{S0}^2}\delta\right)$

Table 1: Phase-velocity parameters in Thomsen’s notation. The parameters r_2 and r_4 of the phase-velocity series can be replaced wavetype-specifically by Thomsen’s (1986) anisotropy parameters ϵ and δ and the ratio of the qP -to- qSV reference phase velocities (Thomsen, 1986; Tsvankin and Thomsen, 1994).

parameter	wavetype	
	$q\grave{P}q\acute{P}$	$q\grave{S}Vq\acute{S}V$
r_4^\dagger	$2 \frac{(\epsilon - \delta) \left(1 + 2 \frac{v_{P0}^2}{v_{P0}^2 - v_{S0}^2} \delta \right)}{(1 + 2\delta)^2}$ $\xrightarrow{\frac{v_{P0}}{v_{S0}} \rightarrow \infty} 2 \frac{\epsilon - \delta}{1 + 2\delta} := 2\eta$	$-2 \frac{\frac{v_{P0}^2}{v_{S0}^2} (\epsilon - \delta) \left(1 + 2 \frac{v_{P0}^2}{v_{P0}^2 - v_{S0}^2} \delta \right)}{\left(1 + 2 \frac{v_{P0}^2}{v_{S0}^2} (\epsilon - \delta) \right)^2}$ $\stackrel{1^{\text{st}} \text{ order}}{\approx} -2 \frac{\frac{v_{P0}^2}{v_{S0}^2} (\epsilon - \delta)}{1 + 4 \frac{v_{P0}^2}{v_{S0}^2} (\epsilon - \delta)} := -2\chi$

Table 2: Phase-velocity parameters of a nearly-isotropic medium in Thomsen's notation: The quadratic term r_2^\dagger vanishes by definition, and the quartic term r_4^\dagger is governed by Thomsen's (1986) anisotropy parameters and the qP -to- qSV ratio of the reference phase velocities. Note Tsvankin and Alkhalifah's (1995) anisotropy parameter η and its newly defined counterpart χ for the $q\grave{S}Vq\acute{S}V$ -wave. Alternatively, select specific ratios of the qP -to- qSV phase velocities or apply Taylor-expansions differently.